Spin-Dependent Perpendicular Magnetotransport through a Tunable $ZnSe/Zn_{1-x}Mn_xSe$ Heterostructure: A Possible Spin Filter?

J. Carlos Egues*

Departamento de Física e Informática, Instituto de Física de São Carlos, Universidade de São Paulo, 13560-970 São Carlos, São Paulo, Brazil

(Received 25 August 1997)

This work addresses spin-dependent magnetotransport in a band-gap-matched $ZnSe/Zn_{1-x}Mn_xSe$ heterostructure. In an external magnetic field the paramagnetic layer behaves as a potential well for spin-down electrons and a potential barrier for spin-up ones. My current-density calculation shows a strong suppression of the spin-up component of the current density for increasing magnetic fields; the total current density is dominated by the spin-down component for $B > 2$ T. This result gives rise to the possibility of devising spin filters relevant for spin-dependent optoelectronics. [S0031-9007(98)06088-8]

PACS numbers: 75.50.Pp, 72.10.–d, 72.90.+y, 84.32.–y

The incorporation of magnetic impurities into semiconductor heterostructures harmoniously combines magnetism and quantum-size effects to uniquely produce exotic new physics. Electrons in Mn-based systems interact with the $3d$ electrons of the localized magnetic moments of the Mn ions via the sp-d exchange interaction [1]. In an external magnetic field this interaction gives rise to a *giant* effective Zeeman effect which lifts the degeneracy of the spin-up and spin-down electron and hole states. This is the essence of the spin-dependent phenomena in these systems [2].

Since the theoretical proposal by von Ortenberg [3] of the so-called spin superlattice—a Mn-(or Fe-)based superlattice where there occurs exchange-induced *spatial* spin segregation of electrons and holes—and its subsequent experimental realization by Dai *et al.* [4] and Chou *et al.* [5], many creative experimental works have been done by exploiting spin-dependent phenomena. These encompass magneto-optical pump-and-probe spectroscopy studies [6] and, more recently, Hall-effect measurements in spin-polarized two-dimensional electron gases in novel Mn-based systems [7]. Transport measurements complement magneto-optical ones thus providing a more complete description of the spin-dependent physics in Mn-based heterostructures.

Electronic *spin filters*, i.e., devices which would produce spin-polarized injection currents, are relevant for spin-dependent optoelectronics [8]. Spin filters could be used to devise circularly polarized light sources, e.g., light emitting diodes and lasers, operating with polarized injection currents.

In this Letter, I report the *first* theoretical investigation on electronic spin filtering in perpendicular transport through a magnetic-field tunable $ZnSe/Zn_{1-x}Mn_xSe$ heterostructure [Fig. 1(a)]. The concentration of Mn in the "paramagnetic" layer is chosen so that in the absence of an applied magnetic field, the conduction and valence band offsets are nearly zero [4] [see Fig. 1(b)]. This unique matching of band gaps is possible only because, at low concentrations, the energy gap of the $Zn_{1-x}Mn_xSe$ presents a characteristic bowing [2] as a function of Mn concentration x.

The heterojunction I study is realistic. In fact, it is similar to the $ZnSe/Zn_{1-x}Mn_xSe$ spin superlattice experimentally realized in Ref. [4]. Because of the sp-d exchange interaction, an external magnetic field modulates the potential profile seen by a traversing electron (or heavy hole) in a spin-dependent fashion. As shown in Fig. 1(c), spin-down electrons see a quantum *well* while spin-up ones see a *barrier*. This simple system generalizes the usual quantum mechanics textbook problems of particles impinging on square potentials in that, here, the potential is both a barrier *and* a well. The electron transmission and reflection coefficients are now spin dependent, Figs. 2(a)–2(f).

I have calculated the electron current density through the system shown in Fig. 1(a) as a function of an external

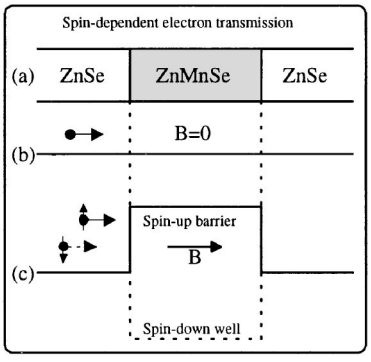

FIG. 1. Band-gap-matched $ZnSe/Zn_{1-x}Mn_xSe$ heterostructure and its conduction-band profile. An electron traversing the system (a) sees a flat (i.e., zero band offsets) potential (b) in the absence of a magnetic field. For nonzero magnetic fields, the s-d exchange interaction gives rise to a spin-dependent potential; spin-up electrons see a *barrier* while spin-down ones a *well* [solid and dashed profiles in (c)]. By increasing the magnetic field the spin-up electrons are *filtered out*, thus producing a spin-polarized transmitted flux.

 0031-9007/98/80(20)/4578(4)$15.00

magnetic field. The total current density is composed of spin-up and spin-down components [Figs. 3(a) and 3(b)]. My calculation includes Landau-level quantization. For increasing magnetic fields and small emitter Fermi energies (e.g., 5 meV, which corresponds to an electron density $\sim 10^{17}$ cm^{-3}), I find (i) strong suppression of the spin-up component of the current density—the total current being dominated by the spin-down component—for fields larger than 2 T, (ii) noticeable resonances in the spin-down component of the current corresponding to the many *quasibound states* that are being pulled into the well which becomes deeper with B, (iii) an essentially structureless exponential decay of the spin-up current, since the barrier height is increasing with B, and (iv) fine Landau-level oscillations in the derivatives of both the spin-up and spin-down currents [Figs. 3(a) and 3(b)]. Point (i) is the relevant feature for *spin filtering*.

Within mean field and for a magnetic field along the z axis, the s-d exchange interaction gives rise to a spin-dependent potential $V_{\sigma_z}(z) = -x\langle S_z\rangle N_0\alpha\sigma_z\Theta(z)\Theta(L - z)$ in the Hamiltonian of the system. Here, x is the Mn concentration, $\langle S_z\rangle$ is the thermal average of the Mn spin components along the magnetic field (a 5/2 Brillouin function), $N_0\alpha$ is the electron s-d exchange constant, σ_z is the electron spin components $\pm 1/2$ (or $\uparrow, \downarrow$) along the field, $\Theta(z)$ is the Heaviside function, and L is the width of the $Zn_{1-x}Mn_xSe$ layer.

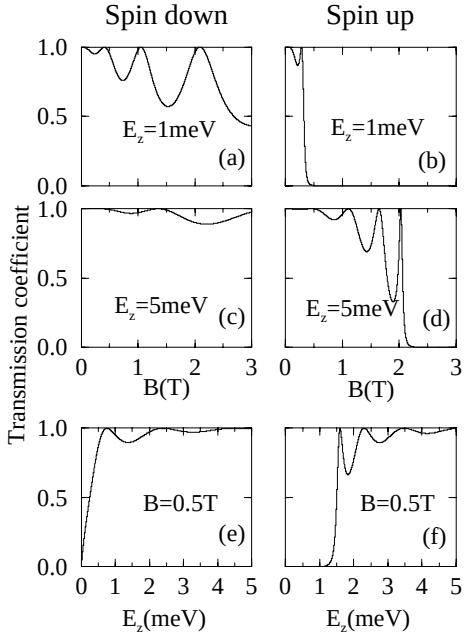

FIG. 2. Spin-dependent transmission coefficients for spin-down and spin-up electrons (left and right panels, respectively) traversing the heterostructure in Fig. 1. The quantum resonances in (a)–(f) correspond to integer numbers of half electron wavelengths fitting within the $Zn_{1-x}Mn_xSe$ layer. Observe the strong suppression of $T_\uparrow(E_z, B)$ for fields larger than a given threshold [>0.5 T in (b) and >2 T in (d)]. This suppression is relevant for *spin filtering*.

In the absence of any kind of electron scattering the motion along the z axis is decoupled from that of the x-y plane. The in-plane motion is quantized in Landau levels with energies $E_n = (n + 1/2)\hbar\omega_c$, where $n = 0, 1, 2, \ldots$ and $\hbar\omega_c = e\hbar B/m_e^* c$ (I assume a single electron effective mass m_e^* throughout the heterostructure. Along the z axis the electrons are characterized by spin-dependent transmission coefficients $T_{\sigma_z}(E_z, B)$, where $E_z = \hbar^2 k_z^2/2m_e^*$ is the energy of a traversing electron with wave number k_z. An expression for $T_{\sigma_z}(E_z, B)$ is readily obtained by replacing with $V_{\sigma_z}(z)$ the one-dimensional potentials in the usual formulas for the transmission coefficients, found in many quantum-mechanics textbooks [9]. The spin-down transmission coefficient is given by

$$T_\downarrow(E_z, B) = \left\{ 1 + \frac{\sin^2\left[\sqrt{\frac{2m_e^*(x|\langle S_z\rangle|N_0\alpha/2 + E_z)}{\hbar^2}}\, L\right]}{4\left(\frac{E_z}{x|\langle S_z\rangle|N_0\alpha/2}\right)\left(\frac{E_z}{x|\langle S_z\rangle|N_0\alpha/2} + 1\right)} \right\}^{-1} . \quad (1)$$

Expressions similar to Eq. (1) hold for $T_\uparrow(E_z, B)$ (there are two, corresponding to: $E_z > x|\langle S_z\rangle|N_0\alpha/2$ and $E_z < x|\langle S_z\rangle|N_0\alpha/2$). Note that the transmission coefficients are now functions of the external magnetic field through $\langle S_z\rangle$.

Figures 2(a)–2(d) show plots of $T_\downarrow(E_z, B)$ and $T_\uparrow(E_z, B)$ (left and right panels, respectively) as a function of B for two incident energies E_z. Figures 2(e) and 2(f) are the usual textbook plots of the transmission coefficients for particles traversing a well and a barrier, respectively, as a function of the incident energy. In all graphs in Figs. 2(a)–2(f) the unity transmission peaks are quantum resonances; they correspond to an integer number m of *half* electron wavelengths $\lambda/2$ fitting within the potential width, i.e., $L = m\lambda/2$ (Fabry-Perot-like interferences) [9].

The exchange-induced resonances in transmission coefficients, for a fixed incident energy E_z, are interesting because they are magnetic-field tunable [Figs. 2(a)–2(d)]. For the spin-down electrons an increasing magnetic field makes the quantum well deeper and deeper. This in turn pulls down (and into the well) the many *quasistationary* states above the well. Every time one of these quasibound states resonates with the energy E_z, the spin-down electron is transmitted with unity probability. Note that the higher E_z the larger the separation between the resonant peaks [cf. Figs. 2(a) and 2(c)]. This happens because the energy difference between two consecutive quasibound energy levels goes with L^{-2}.

For the spin-up electrons the potential barrier becomes higher and higher for increasing magnetic fields. For incident energies $E_z < x|\langle S_z\rangle|N_0\alpha/2$, the spin-up electron wave is evanescent in the paramagnetic layer and the transmission is suppressed. For $E_z > x|\langle S_z\rangle|N_0\alpha/2$, stationary waves exist above the barrier and resonances occur in $T_\uparrow(E_z, B)$. Figure 2(b) shows these two regimes for $E_z = 1$ meV; for $B > 0.5$ T the transmission is suppressed, and for $B < 0.5$ T there is a resonant peak. Similarly, however. for a higher incident energy,

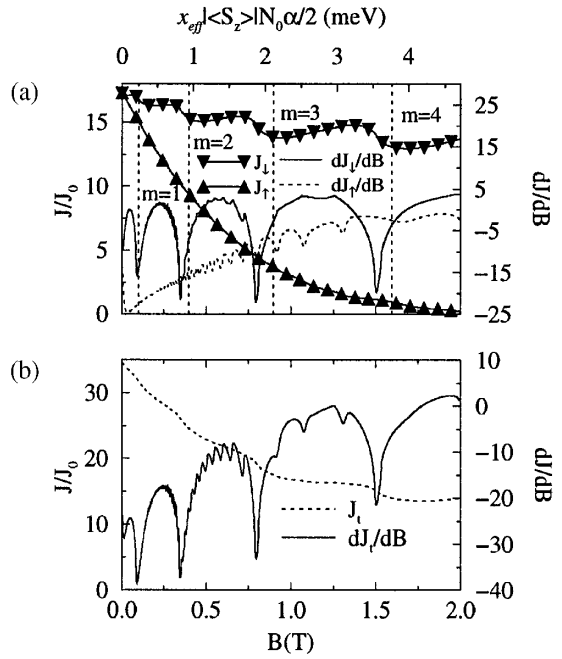

FIG. 3. Calculated current densities and their respective derivatives as functions of the magnetic field and the energy $x_{\rm eff}|\langle S_z\rangle|N_0\alpha/2$, bottom and top x axis, respectively. The spin-down current (triangle down) shows oscillations due to quasibound resonances above the well. These are readily seen in its derivative [solid line in (a)] which presents dips at energies $E_m \approx 0.24m^2$ meV [infinite-well bound states, see dashed vertical lines in (a)]. The spin-up current is structureless and exponentially suppressed for increasing magnetic field (triangle up). The derivatives of both spin-up and spin-down current [dashed and solid lines in (a) especially] exhibit fine oscillations due to Landau quantization. The *total* current density [dashed line in (b)] shows oscillations (spin down) superimposed on an exponential decay (spin up). Its derivative [solid line in (b)] presents both quasibound state resonant dips and the fine Landau-level oscillations. The total current density is dominated by the spin-down component for $B > 2$ T (spin filtering).

Fig. 2(d) displays suppression of the transmission for $B > 2$ T and many resonances for $B < 2$ T. Note also the complementary behavior of Figs. 2(b) and 2(f).

The resonances in the transmission coefficients described above also appear in the current versus magnetic field characteristics of the system. To calculate the spin-dependent current density through the system, I assume that the ZnSe layers in Fig. 1(a) are now emitter and collector attached to external leads. In addition, I assume low enough temperatures so that $T \approx 0$ (the experiments are usually done at 4.2 K). Denoting by $\psi_{n,k_y,k_z}(\mathbf{r})$ the Landau-level eigenstates and by $v_z(k_z) = \hbar k_z/m_e^*$ the z component of the electron velocity, the spin-dependent current density is given by

$$j_{\sigma_z}(\mathbf{r},B) = e \sum_{n,k_y,k_z\geq 0} v_z(k_z) T_{\sigma_z}(k_z,B) |\psi_{n,k_y,k_z}(\mathbf{r})|^2, \quad (2)$$

where $\psi_{n,k_y,k_z}(\mathbf{r}) = \frac{1}{\sqrt{L_y}} \frac{1}{\sqrt{L_z}} e^{ik_y y} e^{ik_z z} \varphi_n(x)$. Here, $\varphi_n(x)$ is the nth harmonic-oscillator eigenfunction centered at $x_0 = -\hbar k_y/m\omega_c$, (L_x) L_y and L_z are normalization constants, and k_y and k_z are the electron wave vectors along the y and z directions, respectively. These scattering states have energies $E_{n,k_z} = (n + 1/2)\hbar\omega_c + \frac{\hbar^2 k_z^2}{2m_e^*}$ (I am neglecting the small contribution $g^*\mu_B B\sigma_z$ to E_{n,k_z}, g^* is the effective electron gyromagnetic ratio).

The *average* spin-dependent current density is defined by

$$J_{\sigma_z}(B) = \frac{e}{V} \sum_{n,k_y,k_z\geq 0} v_z(k_z) T_{\sigma_z}(k_z,B) \int_{-\infty}^{+\infty} |\varphi_n(x)|^2 dx, \quad (3)$$

where $V = L_x L_y L_z$ is the normalization volume. With E_f denoting the emitter Fermi energy, the summation over the discrete Landau levels n and over $k_z \geq 0$ in Eq. (3) must satisfy (i) $0 \leq (n + 1/2)\hbar\omega_c + \frac{\hbar^2 k_z^2}{2m_e^*} \leq E_f$ for an external bias $eV > E_f$, and (ii) $E_f - eV \leq (n + 1/2)\hbar\omega_c + \frac{\hbar^2 k_z^2}{2m_e^*} \leq E_f$ for $eV \leq E_f$. Constraint (i) says that all electrons below E_f contribute to the current density, since $eV > E_f$, while (ii) restricts this contribution to only those electrons with high enough energy. The summation on k_y is equal to $L_x L_y eB/2\pi\hbar c$, i.e., the total number of k_y points. Since the transmission coefficients depend only on k_z and $\varphi_n(x)$ is normalized, Eq. (3) becomes, for $eV \geq E_f$,

$$J_{\sigma_z}(B) = J_0 B \int_0^{E_f - \hbar\omega_c/2} (n_{\max}(B) + 1) T_{\sigma_z}(E_z,B) dE_z, \quad (4)$$

where $n_{\max}(B) = \text{int}(\frac{E_f - E_z}{\hbar\omega_c} - \frac{1}{2})$, with int$(x)$ being equal to the larger integer smaller than or equal to x and $J_0 \equiv e^2/4\pi^2\hbar^2 c$.

Equation (4) is easily evaluated via standard numerical-integration schemes. In this paper, I present results for only the *small-bias* limit, i.e., $eV = E_f \approx 5$ meV. In this regime, I can still use, as a first approximation, the zero-bias transmission coefficients to calculate the current densities. The *total* current density through the heterostructure is $J_t(B) = J_\uparrow(B) + J_\downarrow(B)$. Note that the current densities depend upon B (i) explicity via the factor of B, due to the degeneracy of a Landau level, (ii) through $n_{\max}(B)$, which denotes the maximum number of filled Landau levels for a given E_z, (iii) via $T_{\sigma_z}(E_z,B)$ and (iv) through the upper limit of integration $E_f - \hbar\omega_c/2$ in Eq. (4). In what follows I neglect the weak magnetic-field dependence in (iv) and discuss some interesting resonant structures predicted by Eq. (4).

In all of the graphs I use, $E_f = 5$ meV, $L = 1000$ Å [10], $m_e^* = 0.16m_e$, and an *effective* Mn concentration $x_{\rm eff} = x(1 - x)^{12}$. This effective concentration accounts, in an *ad hoc* way, for some of the antiferromagnetic clustering effects (those due to Mn-Mn pairs) which suppress the low-field paramagnetic response of the system. I do not consider effective temperatures in the argument of the Brillouin function.

Figure 3(a) shows curves of $J_\uparrow(B)$ and $J_\downarrow(B)$, and their respective derivatives, as a function of B. The spin-down

component of the current density displays oscillations as the magnetic field is increased. This behavior is a direct consequence of the resonances in $T_{\downarrow}(E_z, B)$ and is readily seen in the $dJ_{\downarrow}(B)/dB$ vs B curve. This curve shows dips at (potential) energies $E_m = m^2\hbar^2\pi^2/2m_e^*L^2$, $m = 1, 2, 3, \ldots$, which correspond to the *quasibound* state energies of an infinite-well potential. For the parameters used in the simulation, $E_m \approx 0.24m^2$ meV. The dashed vertical lines in Fig. 3(a) mark the positions of the E_1, E_2, E_3, and E_4 energy levels [see top x axis in Fig. 3(a)].

The spin-up current density [triangle up in Fig. 3(a)], is essentially exponentially decaying. This reflects the dominant exponential suppression of $T_{\uparrow}(E_z, B)$ for increasing magnetic fields and $0 \leqslant E_z \leqslant E_f$ [see Figs. 2(b) and 2(d)]. No particular structure is seen in the $J_{\uparrow}(B)$ curve. Its derivative, on the other hand, is much more interesting. In fact, the derivatives of both $J_{\uparrow}(B)$ and $J_{\downarrow}(B)$ present rich fine structures. In the $dJ_{\downarrow}(B)/dB$ vs B curve [solid line in Fig. 3(a)] these fine "resonances" appear superimposed by the quasibound state resonances. These additional oscillations are due to Landau-level quantization which explicitly appears in $J_{\sigma_z}(B)$ through the *discrete* factor $n_{\max}(B)$ in the integrand [see Eq. (4)].

Figure 3(b) shows the *total* current density $J_t(B)$ and its derivative as a function of B (see dashed and solid lines, respectively). The total current density exhibits both the oscillatory behavior and the exponential decay of $J_{\downarrow}(B)$ and $J_{\uparrow}(B)$, respectively. Both the quasibound state resonances and the Landau-level related ones are present in the derivative of $J_{\downarrow}(B)$. The former could, in principle, be seen experimentally by measuring the $J_t(B)$ vs B characteristics of the $ZnSe/Zn_{1-x}Mn_xSe$ heterostructure.

Spin filters.—Note that with $E_f = 5$ meV [11] and for $B \gtrsim 2$ T, $J_t(B)$ is dominated by the spin-down component of the current density, i.e., $J_t(B) \approx J_{\downarrow}(B)$ [see dashed line in Fig. 3(b)]. This very interesting feature enables the generation of spin-polarized injection currents since the heterostructure filters out the spin-up component of the electron current density. This is relevant for devising tunable spin-dependent electronic switches and possibly to the development of a circularly polarized laser [12].

Important points.—Electron-electron (*e-e*) interaction, band bending, and spin-flip processes, all neglected here, reduce the efficiency of spin filtering. Antiparallel-spin *e-e* scattering in the emitter region can excite spin-up electrons to energies above E_f, thus enhancing their transmission probability. Band bending changes the transmission and enhances *e-e* scattering because of charge accumulation in the vicinity of the potential barrier. The *s-d* exchange-induced spin-flip mechanism can be relevant for small barrier heights [13]. A possible way to minimize the *e-e* and *s-d* effects is to use a paramagnetic layer with a higher potential barrier (i.e., $x > 0.05$). Higher barriers suppress both the tunneling of excited spin-up electrons *and* the *s-d* exchange-induced scattering. Band bending effects should be small for filters with a short intrinsic region between the emitter and the paramagnetic layer.

In summary, I have studied perpendicular spin-dependent magnetotransport in tunable ZnSe/$Zn_{1-x}Mn_xSe$ heterostructures. The spin-down current density displays oscillatory behavior for increasing magnetic fields while the spin-up one decays exponentially. These features are easily understood in terms of the usual resonant-transmission picture through square barriers and wells. Additional fine structures, due to Landau quantization, are seen in the derivatives of the current densities. For $B > 2$ T the total current density is dominated by the spin-down component. This feature can be used to devise electronic *spin filters* possibly relevant for spin-dependent optoelectronics. *Optimal* filters should have a high spin-up barrier, a vanishingly small (i.e., very shallow) spin-down well, and a short (if any) intrinsic region separating the emitter and the paramagnetic layer. This design should, in principle, minimize detrimental effects to spin filtering.

I thank L. N. Oliveira and L. Ioriatti for a critical reading of this manuscript and for useful discussions. This work was supported by Fundação de Amparo à Pesquisa do Estado de São Paulo (FAPESP).

*Electronic address: egues@ifsc.sc.usp.br

[1] J. Kossut, Phys. Status Solidi (b) **72**, 359 (1975).
[2] J. K. Furdyna, J. Appl. Phys. **64**, R29 (1988).
[3] M. von Ortenberg, Phys. Rev. Lett. **49**, 1041 (1982).
[4] N. Dai *et al.*, Phys. Rev. Lett. **67**, 3824 (1991).
[5] W. C. Chou *et al.*, Phys. Rev. Lett. **67**, 3820 (1991).
[6] S. Crooker *et al.*, Phys. Rev. Lett. **75**, 505 (1995); J. Levy *et al., ibid.* **76**, 1948 (1996); S. Crooker *et al., ibid.* **77**, 2814 (1996).
[7] I. P. Smorchkova *et al.*, Phys. Rev. Lett. **78**, 3571 (1997).
[8] For a review on spin-polarized transport and its applications, see G. Prinz, Phys. Today **48**, 58 (1995). G. Fasol [Appl. Phys. Lett. **62**, 2230 (1993)] also discusses this subject.
[9] See, for instance, A. Yariv, *An Introduction to Theory and Applications of Quantum Mechanics* (Wiley, New York, 1982), Chap. 4.
[10] I assume the $Zn_{1-x}Mn_xSe$ layer is *coherently strained* (no dislocations). For $x = 0.05$ the relative difference in lattice constants between the ZnSe and the $Zn_{1-x}Mn_xSe$ compounds is about 0.2%.
[11] A substantial suppression of the spin-up component of the current density is possible only if $V_{\uparrow} \geqslant E_f$ for some $B \leqslant B_{\text{sat}}$. Here B_{sat} denotes a *saturation* field for which most of the isolated Mn spins are aligned. For the parameters, I use $E_f \leqslant x_{\text{eff}}|\langle S_z\rangle|N_0\alpha/2 \approx 5$ meV, for $B \approx 2$ T.
[12] Injection currents of either polarization can also be produced with a double-barrier resonant-tunneling structure similar to the one studied by V. I. Sugarov and S. A. Yatskevich [Sov. Tech. Phys. Lett. **18**, 134 (1992)].
[13] Band-structure related mechanisms and spin-orbit coupling are not very efficient spin-flip processes for electrons; see G. Bastard and R. Ferreira, Surf. Sci. **267**, 335 (1992).